JOURNAL OF NEUROTRAUMA 36:1–10 (Month XX, 2019)

DOI: 10.1089/neu.2018.6208

Original Article

Optical Assessment of Spinal Cord Tissue Oxygenation Using a Miniaturized Near Infrared Spectroscopy Sensor

Babak Shadgan,[1,2] Andrew Macnab,[3] Allan Fong,[2] Neda Manouchehri,[2] Kitty So,[2] Katelyn Shortt,[2] Femke Streijger,[2] Peter A. Cripton,[1,4] Eric C. Sayre,[5] Guy A. Dumont,[6] Roberto Pagano,[6] Kyoung-Tae Kim,[7] and Brian K. Kwon[1,2]

Abstract

Despite advances in the treatment of acute spinal cord injury (SCI), measures to mitigate permanent neurological deficits in affected patients are limited. Immediate post-trauma hemodynamic management of patients, to maintain blood supply and improve oxygenation to the injured spinal cord, is currently one aspect of critical care which clinicians can utilize to improve neurological outcomes. However, without a way to monitor the response of spinal cord hemodynamics and oxygenation in real time, optimizing hemodynamic management is challenging and limited in scope. This study aims to investigate the feasibility and validity of using a miniaturized multi-wavelength near-infrared spectroscopy (NIRS) sensor for direct transdural monitoring of spinal cord oxygenation in an animal model of acute SCI. Nine Yorkshire pigs underwent a weight-drop T10 contusion-compression injury and received episodes of ventilatory hypoxia and alterations in mean arterial pressure (MAP). Spinal cord hemodynamics and oxygenation were monitored throughout by a non-invasive transdural NIRS sensor, as well as an invasive intraparenchymal sensor as a comparison. NIRS parameters of tissue oxygenation were highly correlated with intraparenchymal measures of tissue oxygenation. In particular, during periods of hypoxia and MAP alterations, changes of NIRS-derived spinal cord oxygenated hemoglobin and tissue oxygenation percentage corresponded well with the changes in spinal cord oxygen partial pressures measured by the intraparenchymal sensor. Our data confirm that during hypoxic episodes and as changes occur in the MAP, non-invasive NIRS can detect and measure real-time changes in spinal cord oxygenation with a high degree of sensitivity and specificity.

Keywords: animal model; hemodynamics; implantable sensor; NIRS; spinal cord

Introduction

Acute traumatic spinal cord injury (SCI) is a devastating neurological condition, with the potential to result in permanent morbidity, critical complications, a wide range of multi-organ dysfunctions, and significantly reduced quality of life. Acute SCI involves primary and secondary pathological cascades. The first is the disruption of spinal cord that results directly from the initial physical trauma, and the second, which follows in the subsequent hours to days, involves excitotoxicity, ischemia/hypoxia, inflammation, oxidative stress, increased spinal cord intraparenchymal pressure, and, ultimately, further death of neural tissue that survived the initial primary mechanical insult.[1] Neuroprotective treatments aim to limit this secondary SCI cascade and preserve as much spinal cord tissue as possible. The primary neuroprotective treatment options available to reduce secondary SCI and irreversible neuronal damage are urgent surgical decompression of the spinal cord, and the restoration of spinal cord tissue perfusion and oxygenation through aggressive hemodynamic management.[2–5]

Recent evidence suggests that neurological outcome can certainly be influenced by hemodynamic management, making this one of the few opportunities available to improve the lives of individuals who suffer this catastrophic injury.[6] Current clinical practice guidelines

[1]Department of Orthopaedics, Faculty of Medicine, University of British Columbia, Vancouver, British Columbia, Canada.
[2]International Collaboration on Repair Discoveries (ICORD), Vancouver, British Columbia, Canada.
[3]Stellenbosch Institute for Advanced Study, Wallenberg Research Centre, Stellenbosch, South Africa.
[4]Orthopaedic and Injury Biomechanics Group, Departments of Mechanical Engineering and Orthopaedics and School of Biomedical Engineering, UBC, Vancouver, British Columbia, Canada.
[5]Arthritis Research Canada, Richmond, British Columbia, Canada.
[6]Department of Electrical and Computer Engineering, University of British Columbia, Vancouver, British Columbia, Canada.
[7]Department of Neurosurgery, School of Medicine, Kyungpook National University, Kyungpook National University Hospital, Daegu, South Korea.

for managing acute SCI patients recommend that mean arterial pressure (MAP) be augmented to 85–90 mm Hg for the first week post-injury in an effort to improve blood flow and oxygenation to the injured spinal cord.[4–6] However, although such treatment offers one of the few opportunities available to improve outcome after SCI, there is currently no clinical method for monitoring tissue oxygenation within the injured cord continuously by direct and non-invasive measurement. Consequently, when vasopressor agents are used to increase MAP for example, there is no way to measure how this affects regional blood flow and oxygenation within the spinal cord. For this reason, developing a method to continuously monitor spinal cord hemodynamics and oxygenation with accurate, real-time measurements would aid the ability of clinicians to optimize MAP during the early post-injury period and reduce the risk of tissue ischemia and hypoxia contributing to secondary injury.

Near-infrared spectroscopy (NIRS) is a well-established optical technology with a long history of clinical application for monitoring regional oxygenation in various tissues, especially in the brain and skeletal muscles.[7–9] NIRS functions by transmitting light photons in the near-infrared (NIR) spectrum (wavelengths $\sim$700–1000 nm) into tissue, where chromophores, such as oxygenated (O_2Hb) and deoxygenated hemoglobin (HHb), absorb NIR photons in a wavelength-dependent manner.[10,11] In addition to monitoring changes in the concentration of O_2Hb, HHb, and their sum, total hemoglobin (THb) in real time, by using multiple light sources and photodetectors configured in a spatially resolved (SR) configuration, NIRS systems can also provide an absolute measure of tissue oxygenation level (TOI%).[12] In multi-wavelength (MW) configuration, using a single MW light source and one photodetector, changes in tissue oxygen delivery, consumption, and utilization can also be derived from variations in concentration of O_2Hb and HHb, and TOI%.[13–15] Additionally, changes in THb reflect variations in blood volume, a variable of tissue hemodynamics indicative of local blood accumulation in the microcirculation.[16,17]

The aim of this study was to investigate the feasibility of using a custom-made miniaturized MW-NIRS sensor system for direct transdural measurement and real-time monitoring of spinal cord tissue oxygenation in a large animal model of acute SCI, and to evaluate the accuracy of the system's measurement in response to episodes of ventilatory hypoxia and alterations in MAP.

Methods

The previously described pig model of thoracic SCI developed by our laboratory was used for this study.[18] The spinal cord anatomy, cardiovascular system, and vasculature of the pig share many similarities with humans, thus making this model suitable for studying regional tissue hemodynamics after SCI.[19,20] Nine anesthetized adult female Yorkshire pigs, weighing between 25 and 30 kg, were studied. All surgical and experimental procedures performed were approved by the University of British Columbia (UBC) Committee on Animal Care and conformed to the regulations and guidelines of the Canadian Council on Animal Care and the US Army Medical Research and Materiel Command Animal Care and Use Review Office. The anesthesia/analgesia protocols for these procedures are those established at the UBC Center for Comparative Medicine.[21] Animals were anesthetized during the entire protocol and then euthanized at the end of the experiment without any recovery of consciousness.

Near-infrared spectroscopy instrumentation

The custom NIRS sensor that was developed for our study uses a miniaturized optode ($4\times10\times20$ mm), where one single MW surface-mount-device, light-emitting diode with five wavelengths (660, 730, 810, 850, and 950 nm), and an output power of 2 mW, is linked to a single photodetector. They are configured to give an interoptode distances of 10 mm. The sensor was covered by a clear silicon shield to protect it from blood and other fluids. The sensor was designed to be small enough to rest directly on the dural surface of the spinal cord, while connected by a flexible biocompatible multi-branch shielded wire to a compact MW-NIRS system that was placed outside the animal.

The NIRS system utilized a continuous-wave, time-multiplexing configuration, with a mathematical algorithm to translate light attenuation for each wavelength absorbed by O_2Hb and HHb chromophores to their relative concentration changes. The resulting relative concentration changes are the product of scaling the absolute concentration changes by an undetermined scaling factor. This factor, which is called the differential pathlength, is the average distance a photon travels between the source and detector through the tissue. The extinction coefficients were referenced from the literature.[22] By increasing the number of wavelengths (i.e., to more than the conventional two wavelengths), and solving for multiple optical density equations at each wavelength,[15] our MW-NIRS system provides more-accurate measurement of tissue O_2Hb and HHb. The algorithm used is derived from the modified Beer-Lambert Law; THb and Hb difference [Hbdiff = (O_2Hb) – (HHb)] are also calculated. Hbdiff is a NIRS parameter of tissue oxygenation.[23] The NIRS system also calculates the TOI%, which is an absolute measure of tissue oxygenation status. This is done by a second algorithm, which uses the light attenuation of the five wavelengths.

Animal and surgical preparation

Animals were prepared for surgery as previously described.[21] Arterial oxygen saturation (SaO_2) and heart rate (HR) pulsation were monitored with a pulse oximeter (8600 V; Nonin Medical Inc., Plymouth, MN) attached to the animal's ear. Ventilation was set at 17 breaths per minute, and the animal was initially oxygenated with a combination of 1.4 L (70%) of nitrogen and 0.6 L (30%) of oxygen. The left jugular vein and carotid artery were exposed by blunt dissection. A 20-gauge catheter was inserted into the carotid artery and connected to a fluid-filled pressure transducer to yield invasive MAP throughout the experiment. The jugular vein was catheterized for infusion of norepinephrine (NE) and nitroprusside (NP) to purposefully manipulate MAP. The right femoral artery and vein were also exposed and catheterized for collecting arterial and blood samples for blood gas (BG) analysis.

After surgical preparation, the animal was positioned into a prone position. The posterior spine was then surgically exposed between the T4–L3 spine levels. The T9, T10, and T11 pedicles were cannulated and instrumented with 3.5×25 mm polyaxial screws (Vertex screws; Medtronic, Memphis, TN), followed by a laminectomy at the T5–L1 levels to expose the dura and spinal cord. Before SCI, a total of three intraparenchymal (IP) sensors were inserted through the dura into the spinal cord at T11 for the assessment of blood flow, partial pressure of oxygen (NX-BF/OF/E; Oxford Optronix, Oxford, UK), hydrostatic pressure (FOP-LS-NS-1006A; FISO Technologies Inc., Harvard Apparatus, Quebec, QC, Canada), and metabolic changes[21,24] (CMA11, CMA Microdialysis; FISO Technologies Inc., Harvard Apparatus). IP sensors were advanced at a 45-degree angle, to a cord depth of 4 mm, with the sensor tips approximately 12 mm caudal from the anticipated edge of the impactor.[21] A custom-made platform, with precision-drilled holes, positioned above the cord and secured to the spine by 3.5-mm titanium rods (Medtronic) and pedicle screws (Medtronic) at T9, T11, T12, and T14, served as a guide for direct placement of sensors into the cord.[21] Accurate sensor placement was verified by ultrasound imaging (L14–5/38, 38-mm linear array probe,

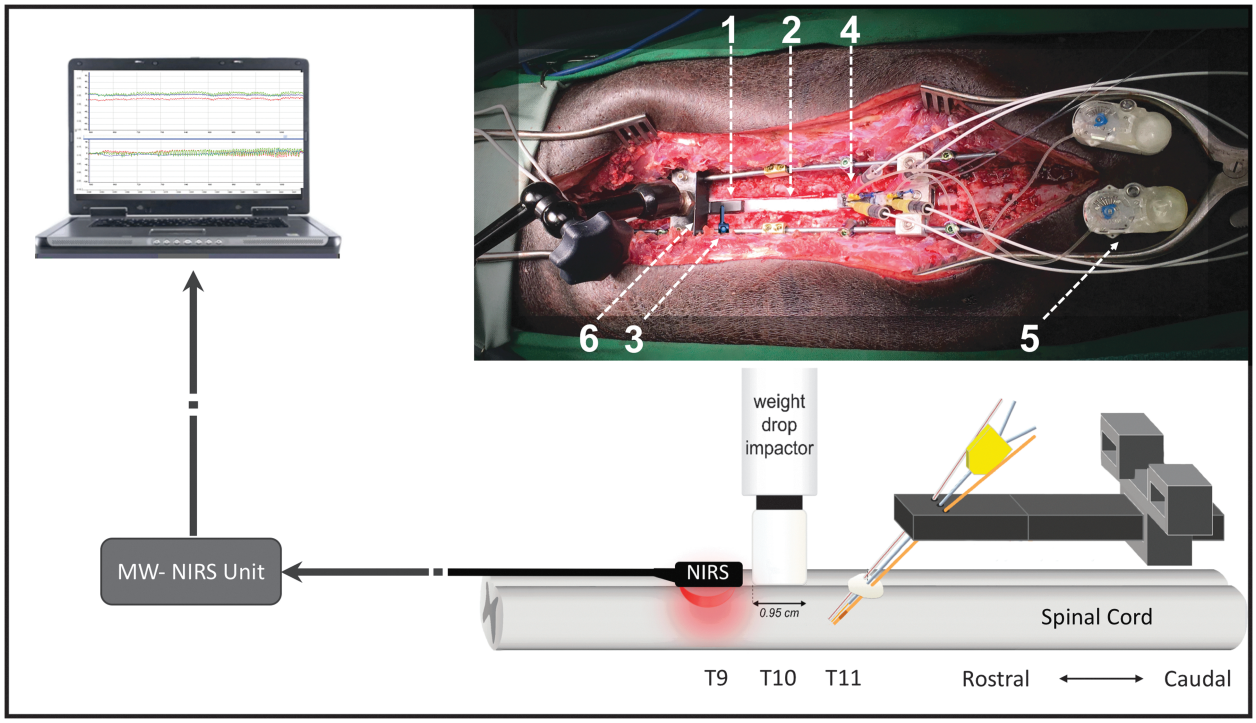

FIG. 1. The custom-made MW-NIRS sensor (1) placed and fixed on the spinal cord at T9 (2) using a cross-connector (3), and invasive IP sensors (4) inserted into the spinal cord at T11. The sensor is connected to the NIRS system using a wire for real-time data collection, storage, and visualization on a laptop computer. Microdialysis probes connected to miniature infusion pumps (5) allowed for the collection of dialysate samples every 10 min. An articulating arm (6) that is attached to the titanium bars positions the impact device. MW, multi-wavelength; NIRS, near infrared spectroscopy. Color image is available online.

Ultrasonix RP; BK Ultrasound, Richmond, British Columbia, Canada). After placement of the IP sensors, the NIRS sensor was placed transdurally at the T9 level and secured with a cross-connector (Fig. 1). The wires of all sensors were brought out of the surgical field, fixed over the back of the animal, and connected to their respective monitoring units.

Data acquisition

IP blood flow and oxygen partial pressure sensors, connected to the Oxyflo/Oxylite monitors (Oxford Optronix) were recorded continuously at a sampling rate of 100 and 1 Hz, respectively. IP pressure sensors were connected to a signal conditioner mounted on a multi-channel chassis (FISO Technologies Inc., Harvard Apparatus) and sampled at 100 Hz. All three parameters were collected by a PowerLab data acquisition device running LabChart software (v7.3.8; ADInstruments Inc., Colorado Springs, CO). Microdialysis samples were collected by a miniature infusion pump every 10 min and analyzed using the Iscus^{Flex} Microdialysis Analyzer (M Dialysis, Stockholm, Sweden) for measuring intracellular lactate and pyruvate concentration levels and calculating lactate-to-pyruvate ratio (L/P ratio), a well-recognized indicator of tissue hypoxia. A laptop computer with custom software was used to collect and record NIRS signals at 100 Hz and to analyze and display tissue O_2Hb, HHb, THb, Hbdiff, and TOI% graphically in real time.

Spinal cord injury procedure

An articulating arm (660; Starrett, Athol, MA) was fixed to the T9-, T10-, and T11-positioned pedicle screws with titanium rods (Fig. 1). This arm positions in place the impact device, which consists of an impactor (diameter, 0.953 cm) fitted with a load cell (LLB215; Futek Advanced Sensor Technology, Irvine, CA) that slides down a guide rail equipped with a Balluff Micropulse® linear position sensor (BTL6-G500-M0102-PF-S115; Balluff Canada Inc., Mississauga, ON, Canada) to record the force and impactor position (from which displacement and velocity were determined). Immediately after the weight-drop contusion injury (weight, 50 g; height, 50 cm), sustained compression was maintained on the contused spinal cord for 30 min by placing an additional 100-g mass onto the impactor (150 g total). The experimental setup is shown in Figure 1.

Experimental protocol

Once the placement of IP and NIRS sensors were finalized and all parameters stabilized, a 90-min baseline recording was allowed before beginning serial episodes of hypoxia and MAP alterations before and after inducing an acute SCI at T10. First, an episode of mild hypoxia was induced by increasing the N_2:O_2 ratio until the animal's SaO_2 dropped to 80%, after which the gas proportion was returned to a 70:30 mix. Next, an episode of severe hypoxia was induced by a complete removal of assisted breathing by the ventilator until the animal's SaO_2 dropped to 70%, followed by a return to normal ventilated respiration on the nitrogen-oxygen gas mix. A recovery period of 30 min followed each hypoxic episode to allow cord measurements to return to baseline levels. After a contusion-compression SCI, the cord was challenged again with another series of hypoxic episodes, with recovery periods in between. Additionally, the effects of MAP alterations were examined. MAP was elevated by 20 mm Hg with the infusion of NE and a decrease of 20 mm Hg achieved by infusion of NP. As with hypoxic challenges, a 30-min recovery period was given between MAP

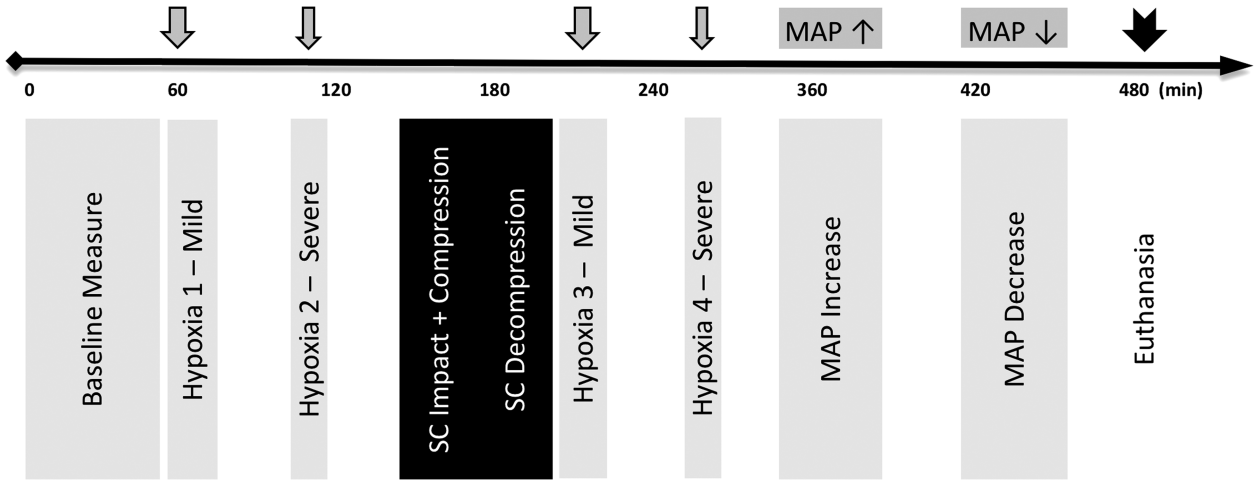

FIG. 2. Experimental protocol, including: two episodes of mild (SaO_2 80%) and severe (SaO_2 70%) hypoxia, SCI and sustained cord compression, cord decompression, post-SCI mild (SaO_2 %80), and severe (SaO_2 %70) hypoxia episodes followed by two episodes of MAP increase and decrease. MAP, mean arterial pressure; SaO_2, oxygen saturation; SC, spinal cord; SCI, spinal cord injury;

alterations to allow cord measurements to return to baseline. NIRS measures of spinal cord tissue oxygenation (O_2Hb, HHb, Hbdiff, and TOI%) and hemodynamics (THb) were compared against the ''gold-standard'' IP measures of perfusion (spinal cord blood flow; SCBF), oxygenation (oxygen partial pressure; PO_2), oxidative cellular metabolism (L/P ratio), and cord pressure (hydrostatic pressure, SCP [spinal cord pressure]) throughout the entire experiment[21] (Fig. 2). Arterial and venous blood were collected for BG analysis at the end of the baseline period, the peak of the severe hypoxic episodes, and at the end of the 30-min post-hypoxia recovery periods.

Statistical analysis

All data, including NIRS measures of spinal cord chromophore concentrations (O_2Hb, HHb), spinal cord IP measures (PO_2, SCBF, SCP, and L/P ratio), and vital signs (SaO_2, HR, and respiratory rate) were recorded continuously during the experimental interventions and recovery periods. The raw optical data were converted into changes in NIRS parameters (O_2Hb, HHb, THb, and Hbdiff) and TOI% calculated by the NIRS software.

Arterial and venous BG analysis was used for calculation of capillary oxygen saturation percentage ($S_{cap}O_2$) levels, based on a reference ratio between the arterial (25%) and venous contribution (75%) to the signal.[25] $S_{cap}O_2$ measures at baseline, acute hypoxia peak, and recovery time were compared with changes of PO_2 as well as NIRS-derived oxygenation parameters (O_2Hb, HHb, Hbdiff, and TOI%) during the same episodes.

Changes in each variable (spinal cord NIRS-derived O_2Hb, HHb, THb, Hbdiff, and TOI% and spinal cord IP, PO_2, SCBF, SCP, and L/P ratio) during each event (hypoxia 1, hypoxia 2, spinal cord [SC] decompression, hypoxia 3, hypoxia 4, MAP increase, and MAP decrease) were compared to 0 using the Wilcoxon signed-rank test to determine statistical significance of each given change. Pearson correlation coefficients were calculated to establish the pair-wise relationships between the IP and NIRS changes during episodes of induced hypoxia and MAP alterations. Combined-intervals (excluding SCI/decomp) sensitivity and specificity of NIRS parameters for predicating positive and negative changes of PO_2 and SCBF were performed. Data are presented as means ± standard error of the mean (SEM) and the level of significance set at $p < 0.05$ for all statistical analysis and comparisons. Data were analyzed using SAS software (v9.4; SAS Institute Inc., Cary, NC).

Results

Nine anesthetized adult female Yorkshire pigs, with mean weight of 27.9 ± 1.34 kg, were studied. NIRS-derived measures of SC oxygenation and hemodynamics (O_2Hb, HHb, Hbdiff, TOI%, and THb), measured by the customized miniature MW sensor, were successfully monitored during experimental interventions in all 9 animals. NIRS sensor placement and continuous monitoring did not result in any health complications.

Spinal cord injury

Average peak force applied to the exposed spinal cord ($n = 9$) was 4964.2 ± 117.3 kdynes with an impulse of 17.78 ± 0.25 kdyne/sec. The impactor's tip traveled 7.9 ± 0.25 mm from initial contact with the exposed dura with a velocity of 2978.8 ± 23.08 mm/sec at impact. Individual biomechanical impact parameters of the animals are presented in Table 1.

Intraparenchymal parameters

Changes in SC PO_2 were statistically significant during all episodes, and changes of SCBF were significant during both episodes

Table 1. Measures of Weight and Injury Parameters

Animal #	*Body weight (kg)*	*Impulse (kdynes*s)*	*Impact velocity (mm/s)*	*Displacement (mm)*	*Force cord (kdynes)*
1	31.0	17.22	2959.74	8.61	4768.75
2	25.0	18.89	3026.98	6.20	4870.88
3	26.0	16.34	3017.17	7.83	4775.92
4	36.0	17.37	2962.98	8.48	4794.28
5	28.0	18.03	3004.94	7.66	4674.63
6	23.0	18.09	3027.20	7.85	5743.95
7	29.5	17.81	2975.10	7.91	4764.81
8	24.0	17.84	2803.40	7.51	4937.32
9	29.0	18.40	2995.94	8.62	5347.63
Mean	**27.9**	**17.78**	**2978.80**	**7.90**	**4964.20**
SEM	**1.34**	**0.25**	**23.08**	**0.25**	**117.30**

SEM, standard error of the mean.

Table 2. Changes of Spinal Cord Oxygen Partial Pressure, mm Hg (PO_2); Spinal Cord Blood Flow, Arbitrary Perfusion Unit (SCBF); Spinal Cord Pressure, mm Hg (SCP); and Percentage Changes of Lactate to Pyruvate Ratio (L/P Ratio) During Episodes of the Experiment (N = 9)

	ΔPO_2 *(mm Hg)*	$\Delta SCBF$ *(APU)*	ΔSCP *(mm Hg)*	$\%\Delta L/P$ *(%)*
Hypoxia 1	−17.93 ± 2.35*	21.88 ± 13.05	0.15 ± 0.15	−0.96 ± 0.42
Hypoxia 2	−19.85 ± 3.18*	0.17 ± 11.81	0.49 ± 0.38	−0.39 ± 0.84
SC decompression	14.44 ± 5.01*	62.06 ± 49.86	−8.36 ± 3.19*	−79.69 ± 30.65*
Hypoxia 3	−13.50 ± 4.43*	23.33 ± 21.08	−0.04 ± 0.54	−10.20 ± 2.86
Hypoxia 4	−16.45 ± 4.12*	−9.47 ± 11.28	0.10 ± 0.32	−1.97 ± 0.98
MAP increase	9.53 ± 3.33*	49.61 ± 14.51*	1.20 ± 1.06	−3.22 ± 0.97*
MAP decrease	−14.74 ± 5.02*	−58.92 ± 20.19*	1.64 ± 0.41*	6.05 ± 2.11*

All values are mean ± standard error of the mean.
*Measures with significant changes ($p < 0.05$).
SC, spinal cord; MAP, mean arterial pressure; APU, arbitrary perfusion units.

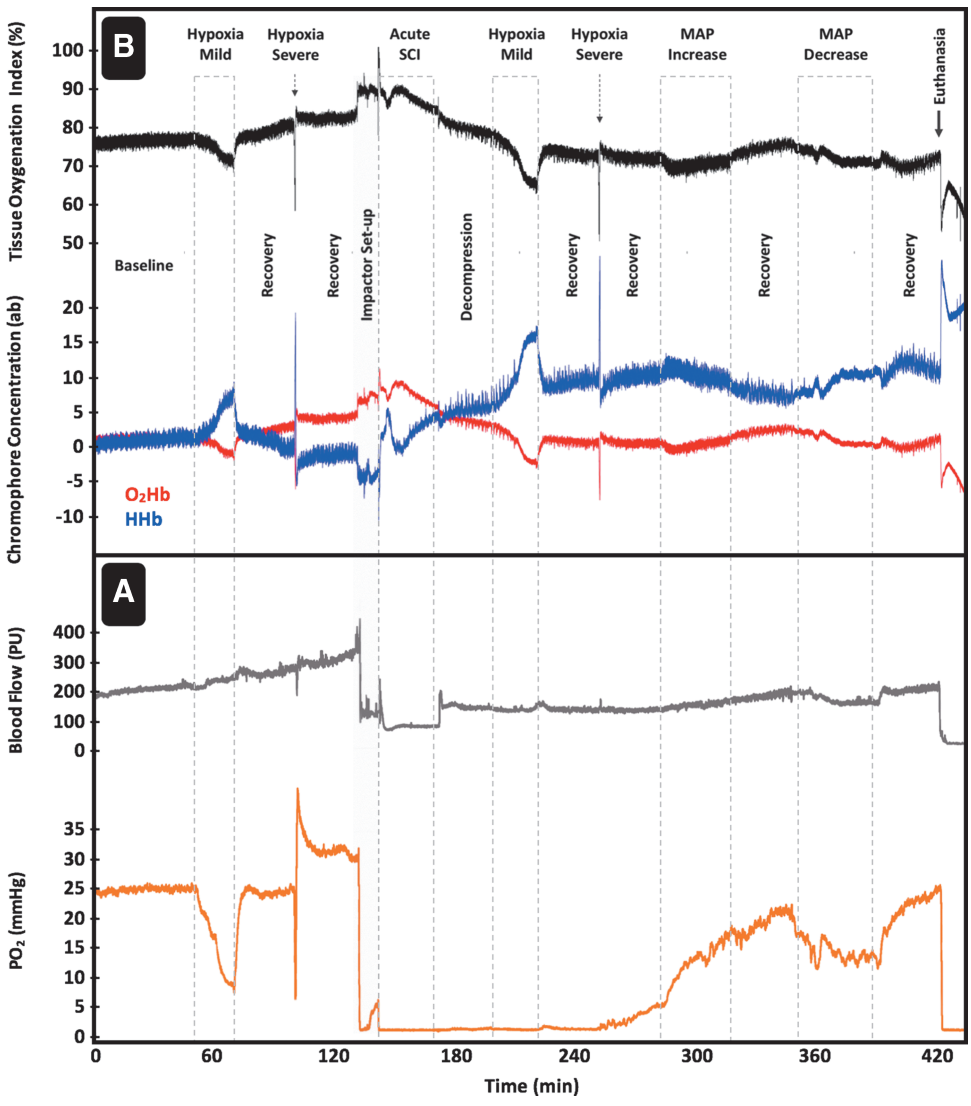

FIG. 3. (**A**) Changes of IP-derived SCBF and PO_2 and (**B**) changes of NIRS-derived O_2Hb, HHb, and TOI%, during the entire experimental protocol in animal #3. In this animal, PO_2 dropped to zero upon the impact and failed to recover for close to 4 h (~130–250 min). It is while changes of O_2Hb, HHb, and TOI% were distinctive during all episodes. Significant changes of parameters during impactor setup were attributed to the severe emission of the surgical light during the setup. ab, arbitrary; HHb, deoxygenated hemoglobin; IP, intraparenchymal; MAP, mean arterial pressure; NIRS, near infrared spectroscopy; O_2Hb, oxygenated hemoglobin; PO_2, oxygen partial pressure; PU, perfusion unit; SCBF, spinal cord blood flow; SCI, spinal cord injury; TOI%, tissue oxygenation percentage. Color image is available online.

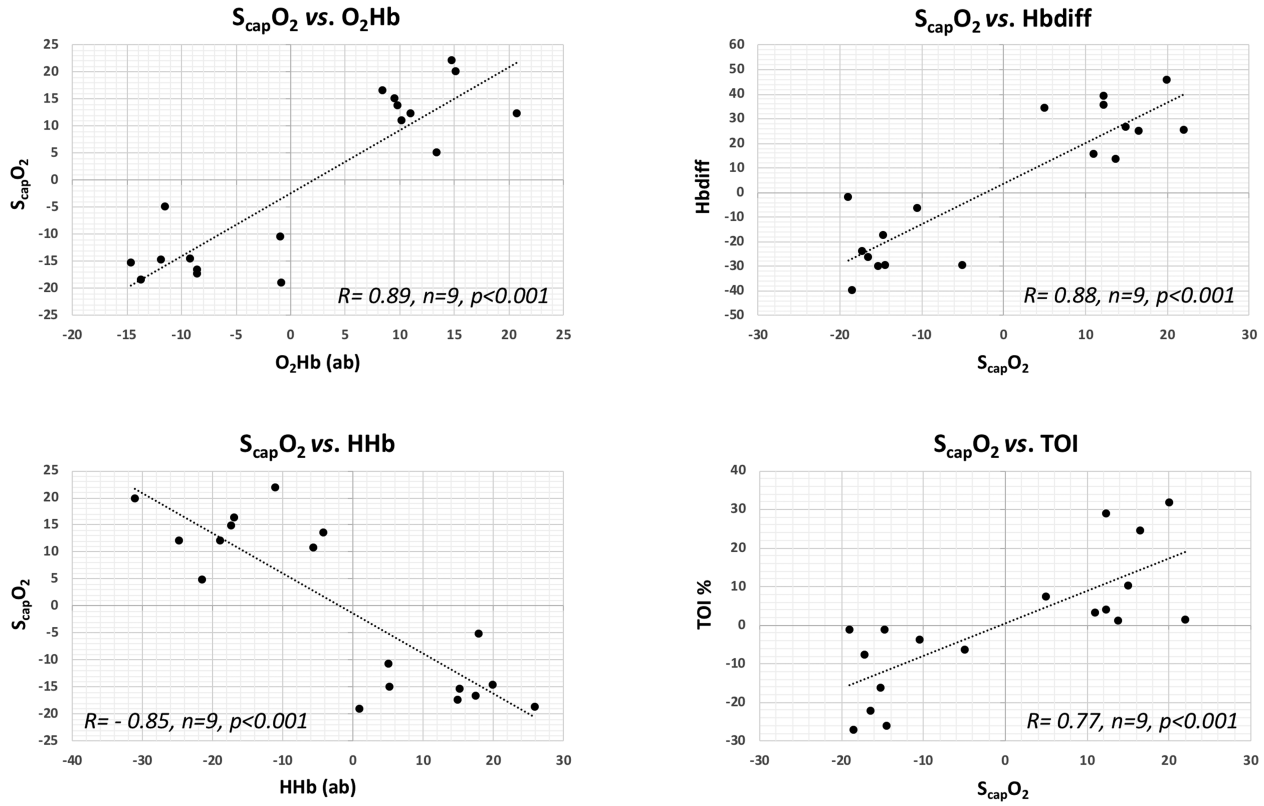

FIG. 4. Pearson correlation analysis between $S_{cap}O_2$ and NIRS-derived O_2Hb, HHb, Hbdiff, and TOI%. ab, arbitrary; Hbdiff, hemoglobin difference; HHb, deoxygenated hemoglobin; NIRS, near infrared spectroscopy; O_2Hb, oxygenated hemoglobin; $S_{cap}O_2$, capillary oxygen saturation percentage; TOI%, tissue oxygenation percentage;

where MAP was increased or decreased. SCP was significantly changed after cord decompression and during when MAP decreased. Percentage changes of L/P ratio were significant after cord decompression and during MAP alterations (Table 2). A representative example of changes of PO_2 and SCBF during sequential experimental interventions is shown in Figure 3A.

Near-infrared spectroscopy parameters

The Pearson correlation analysis, combined-intervals correlation between $S_{cap}O_2$, and NIRS-derived spinal cord O_2Hb, HHb, Hbdiff, and TOI% showed that correlations between $S_{cap}O_2$ and O_2Hb, HHb, Hbdiff, and TOI% were "$R=0.89$, $n=9$, $p<0.001$," "$R=0.85$, $n=9$, $p<0.001$," "$R=0.88$, $n=9$, $p<0.001$," and "$R=0.77$, $n=9$, $p<0.001$" respectively (Fig. 4). The correlation between $S_{cap}O_2$ and PO_2 was also analyzed ($R=0.88$, $n=9$, $p<0.001$).

Changes in NIRS-derived O_2Hb, HHb, Hbdiff, and TOI% during each experimental intervention are shown in Table 3. Changes in TOI% were statistically significant during all events. Changes in spinal cord O_2Hb and Hbdiff were statistically significant during all episodes of hypoxia and alterations in MAP. A representative figure of NIRS parameter changes during the experiment is shown in Figure 3B. Changes in THb were significant during pre-SCI hypoxia and increases in MAP.

Chromophore changes occurring when severe hypoxia was induced (SaO_2 reduced to 70%) are shown in Figure 5. This figure illustrates the sensitivity of the MW-NIRS prototype in detecting physiological changes within the SC tissue before, during, and after the hypoxic event.

TABLE 3. CHANGES OF SPINAL CORD O_2Hb, HHb, HBDIFF, AND TOI% DURING EPISODES OF THE EXPERIMENT (N = 9)

	ΔO_2Hb	ΔHHb	$\Delta Hbdiff$	$\Delta TOI\%$	ΔTHb
Hypoxia 1	−4.46 ± 0.68*	7.56 ± 1.26*	−12.03 ± 1.55*	−5.67 ± 1.61*	3.10 ± 1.31*
Hypoxia 2	−8.85 ± 1.67*	13.60 ± 2.71*	−22.45 ± 4.05*	−12.21 ± 3.54*	4.74 ± 1.99*
SC decompression	4.05 ± 7.51	4.38 ± 5.83	−0.33 ± 3.73	10.33 ± 3.34*	8.41 ± 12.93
Hypoxia 3	−10.22 ± 1.79*	10.75 ± 1.31*	−20.96 ± 1.32*	−7.36 ± 2.26*	5.35 ± 2.05
Hypoxia 4	−12.11 ± 1.52*	16.43 ± 1.46*	−28.54 ± 2.05*	−14.23 ± 4.53*	4.34 ± 2.16
MAP increase	6.17 ± 1.48*	−0.19 ± 1.49	6.36 ± 1.86*	1.64 ± 0.33*	5.99 ± 2.32*
MAP decrease	−6.53 ± 2.34*	6.46 ± 1.73*	−12.99 ± 3.21*	−3.97 ± 0.72*	0.09 ± 2.69

All values are mean ± standard error of the mean.

*Measures with significant changes ($p<0.05$).

SC, spinal cord; MAP, mean arterial pressure; O_2Hb, oxygenated hemoglobin; HHb, deoxygenated hemoglobin; Hbdiff, hemoglobin difference; TOI%, tissue oxygenation percentage; THb, total hemoglobin.

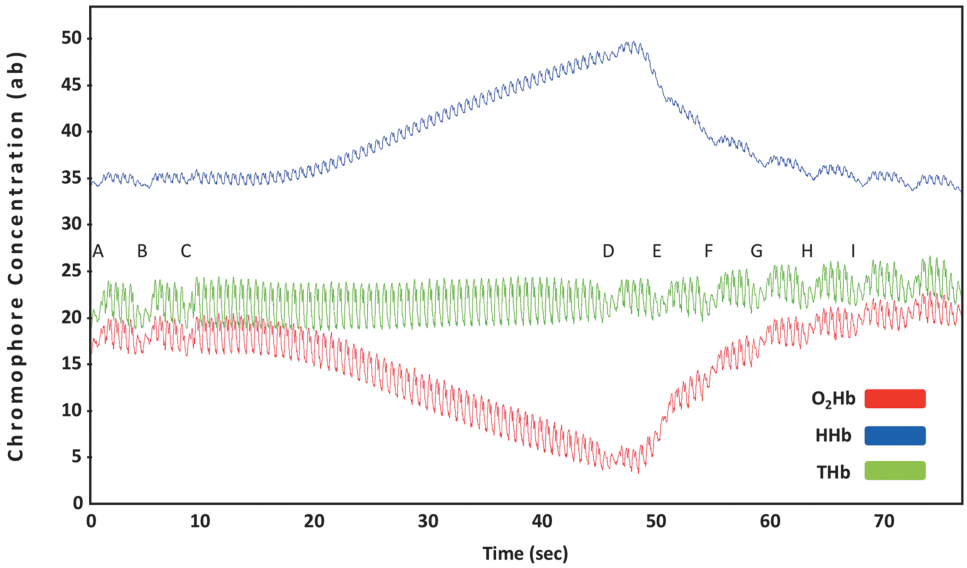

FIG. 5. Changes in spinal cord O_2Hb, HHb, and THb during an episode of severe hypoxia (**C** and **D**). The high-resolution data collected at 100 Hz by the NIRS system utilized in this study capture cardiac pulsations within the spinal cord tissue (i.e. each fine oscillation) and the effect of ventilation on spinal cord tissue oxygenation (i.e., respiratory cycles of A-B, B-C, D-E,…). HHb, deoxygenated hemoglobin; NIRS, near infrared spectroscopy; O_2Hb, oxygenated hemoglobin; THb, total hemoglobin. Color image is available online.

Intraparenchymal versus near-infrared spectroscopy parameters

NIRS-derived changes in HHb, O_2Hb, Hbdiff, and TOI% in the SC after induction of hypoxia, and after reoxygenation, correspond to the changes in spinal cord PO_2 measured by the IP sensor during both periods of hypoxia. Combined-intervals correlation between invasive IP measure of spinal cord PO_2 and non-invasive NIRS measures of spinal cord O_2Hb, HHb, Hbdiff, and TOI% are shown in Figure 6. Combined-intervals sensitivity and specificity of NIRS

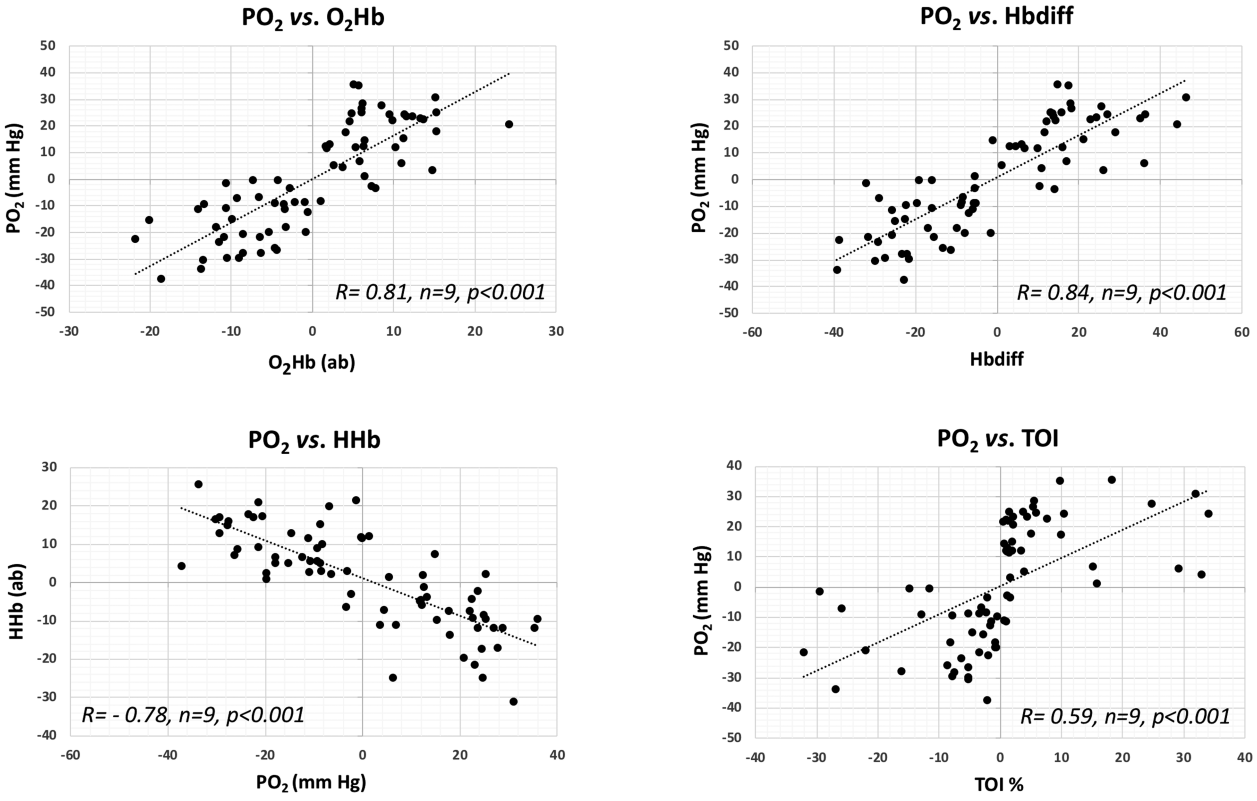

FIG. 6. Pearson correlation analysis between spinal cord PO_2 and NIRS-derived O_2Hb, HHb, Hbdiff, and TOI%. ab, arbitrary; Hbdiff, hemoglobin difference; HHb, deoxygenated hemoglobin; NIRS, near infrared spectroscopy; O_2Hb, oxygenated hemoglobin; PO_2, oxygen partial pressure; TOI%, tissue oxygenation percentage;

Table 4. Combined-Intervals Sensitivity, Specificity, Positive Predictive Value (PPV), and Negative Predictive Value (NPV) for NIRS Parameters Predicating IP Measures of PO_2 and SCBF

NIRS measures predicting positive IP measures	*Sensitivity*	*Specificity*	*PPV*	*NPV*
ΔPO_2 vs. ΔO_2Hb	100.00	92.10	91.89	100.00
ΔPO_2 vs. ΔHHb	14.70	5.26	12.20	6.45
ΔPO_2 vs. $\Delta Hbdiff$	94.12	94.74	94.12	94.74
ΔPO_2 vs. $\Delta TOI\%$	100.00	89.47	89.47	100.00
$\Delta SCBF$ vs. ΔTHb	73.17	50.00	61.22	63.33
NIRS measures predicting negative IP measures				
ΔPO_2 vs. ΔO_2Hb	92.10	100.00	100.00	91.89
ΔPO_2 vs. ΔHHb	5.26	14.70	6.45	12.2
ΔPO_2 vs. $\Delta Hbdiff$	94.74	94.12	94.74	94.12
ΔPO_2 vs. TOI%	89.47	100.00	100.00	89.47
$\Delta SCBF$ vs. ΔTHb	50.00	73.17	63.33	61.22

NIRS, near infrared spectroscopy; IP, intraparenchymal; PO_2, oxygen partial pressure; SCBF, spinal cord blood flow; O_2Hb, oxygenated hemoglobin; HHb, deoxygenated hemoglobin; Hbdiff, hemoglobin difference; TOI%, tissue oxygenation percentage; THb, total hemoglobin.

parameters for predicating positive and negative changes of PO_2 and SCBF are included in Table 4.

Discussion

In this study, we trialed a new optical technique for real-time monitoring of SC tissue oxygenation in acute SCI. Whereas the feasibility of monitoring the SC transcutaneously was reported as early as 2003,[7] direct apposition of a NIRS sensor to the extradural surface of the cord offers greater sensitivity, given the effective depth of penetration of current NIRS techniques ($\sim$15–20 mm) and the complexity of light propagation through multiple layers of non-homogeneous tissue. The miniaturized NIRS sensor we developed has a novel MW configuration suited to the study of SC tissue oxygenation through direct placement over the dura. Our study showed that this NIRS sensor can detect, measure, and monitor changes in SC tissue oxygenation occurring in response to physio- and pharmacological manipulations that alter tissue perfusion and oxygenation in an animal model of acute SCI. High levels of sensitivity and specificity were achieved. The animal model of acute SCI used in this study can be representative of acute traumatic SCI in humans caused by a sudden, high-velocity contusive injury, followed by periods of sustained compression.[19,20] Hence, we suggest that the results of this study can be applicable to clinical situations of acute SCI.

The strong correlations between changes in BG-derived $S_{cap}O_2$ and NIRS measures of SC oxygenation (O_2Hb, HHb, Hbdiff, and TOI%) during episodes of ventilatory hypoxia indicate the ability of this NIRS sensor to monitor changes in SC tissue oxygenation in response to systemic changes alone.

Strong correlations between invasive IP measures of SC oxygenation and non-invasive NIRS measures of SC oxygenation also provide sensitivity and specificity data for the ability of the derived NIRS parameters to predict changes in SC tissue oxygenation, in response to alterations of MAP. Among the NIRS oxygenation parameters, O_2Hb, Hbdiff, and TOI% showed the highest sensitivity and specificity, making them the best NIRS parameters of SC tissue oxygenation. As an absolute measure, independent of O_2Hb and HHb chromophore changes, TOI% appears to be the most reliable parameter for SC tissue oxygenation monitoring. This fact highlights the relevance of using SR or MW configurations of NIRS for monitoring the SC. Given that MW-NIRS requires only one light source and one photodetector, instead of multiple source detectors in conventional SR configuration, MW-NIRS enables the sensors to be smaller in size and therefore more applicable for SC monitoring.

The low sensitivity and specificity of NIRS-derived THb to predict changes of SCBF in our study were likely attributed to the different aspects of tissue hemodynamics each represents. Whereas SCBF, monitored by invasive IP laser Doppler sensor, represents temporal changes of SCBF, THb reflects changes in blood volume within the SC tissue under the NIRS sensor.

Increases in SC THb during first the two pre-SCI episodes of ventilatory-induced hypoxia imply reactive redistribution of blood in response to hypoxia in the intact SC tissue. A similar observation has been described to occur in muscle tissue.[26,27] SCBF did not show any statistically significant changes during hypoxic episodes whereas SC THb increased after 30 min of MAP elevation. Changes in THb were not significant during the 30-min MAP decrease period. A more extended period or larger reduction in the MAP may be necessary for a significant reduction in SC blood volume to occur. Our data indicate that SCBF and THb alone do not provide a complete picture of SC tissue hemodynamics and oxygenation.[21]

The importance of hemodynamic management, and the potential for improving neurologic recovery after acute SCI through cautious elevation of the MAP, has been acknowledged by several researchers.[3–5] It has been shown that improving SC perfusion and oxygenation can result in clinically meaningful neurological improvements in patients with acute SCI.[6] Increasing the MAP, however, may also contribute to a rise in SCP, which, in turn, can compromise SC tissue perfusion and oxygenation. It has also been shown that the MAP value that achieves optimal SC perfusion pressure in one patient may be significantly different from that required by another patient during the first week post-SCI.[28] This finding implies that a ''one-size-fits-all'' MAP target may not be optimal, given that it might improve SC perfusion and oxygenation in some acutely injured patients, whereas it might be harmful in others. If clinicians were given the ability to continuously monitor SC tissue oxygenation in real time, it would enable them to make requirement-based adjustments to a patient's MAP, tailoring the treatment to each individual's need, at any given time.

Tissue oxygenation level is an established adjunct to the measurement of tissue pressure in traumatic brain injury (TBI), and substantial evidence exists to suggest that making a clinical decision based on brain tissue oxygenation level have a positive effect on clinical outcomes in patients with TBI.[29,30] This may further emphasize the significance of direct monitoring of SC tissue oxygenation level in SCI patients during the acute phase of treatment.

Taken together, the outcomes of this study suggest that the transdural MW-NIRS technique described has the potential to fill the void that currently exists for clinicians in their ability to provide optimal hemodynamic care for patients after acute SCI, by offering accurate, non-invasive, real-time, continuous monitoring of SC tissue oxygenation.

We recognize there are limitations to this study. The sample size was small; it was a non-survival animal model of acute SCI; there

were some differences among animals in their cardiorespiratory condition; the duration of the alterations in MAP were short; and the direct application of a MW-NIRS sensor to the dura of the SC is novel. Future studies will include longer episodes of MAP alterations and histological examination of the SC tissue at the NIRS monitoring site.

Although promising, clinical application of this NIRS system must await further technical development and more-extensive clinical trials. To be used at the bedside, the definitive transdural NIRS sensor will need to be a safe, biocompatible, and miniaturized device with a placement mechanism to hold it securely on the dural surface during several days of data collection. We anticipate that the ultimate sensor will be placed at the time of surgical decompression/stabilization surgery after acute SCI and provide real-time monitoring intraoperatively and through the first week post-injury. It will also need to be designed so that it can be easily and safely removed from the patient at the clinician's discretion. The clinical value of having a direct real-time measurement of SC tissue oxygenation and hemodynamics by NIRS, as a means of optimizing patient care and improving neurological outcome in SCI patients, warrants further research and trials.

Acknowledgments

This study was supported by a Translational Research Award from the United States Department of Defense, Spinal Cord Injury Research Program, and an ICORD Seed Grant from the Blusson Integrated Cures Partnership. The authors gratefully acknowledge technical expertise and contributions of Dr. Behnam Molavi in design and development of the NIRS prototypes. The authors also acknowledge expertise and collaborations of the team of veterinarians and animal care technicians at the UBC Center for Comparative Medicine (CCM). B.S. holds a Scholar Award from the Michael Smith Foundation for Health Research. B.K.K. is the Canada Research Chair in Spinal Cord Injury and the Dvorak Chair in Spine Trauma.

Author Disclosure Statement

No competing financial interests exist.

References

1. Kwon, B. K., Tetzlaff, W., Grauer, J.N., Beiner, J., and Vaccaro, A.R. (2004). Pathophysiology and pharmacologic treatment of acute spinal cord injury. Spine J. 4, 451–464.
2. Kong, C.Y., Hosseini, A.M., Belanger, L.M., Ronco, J.J., Paquette, S.J., Boyd, M.C., Dea, N., Street, J., Fisher, C.G., Dvorak, M.F., and Kwon, B.K. (2013). A prospective evaluation of hemodynamic management in acute spinal cord injury patients. Spinal Cord 51, 466–471.
3. Consortium for Spinal Cord Medicine. (2008). Early acute management in adults with spinal cord injury: a clinical practice guideline for health-care professionals. J. Spinal Cord Med. 31, 403–479.
4. Casha, S., and Christie, S. (2011). A systematic review of intensive cardiopulmonary management after spinal cord injury. J. Neurotrauma 28, 1479–1495.
5. Ryken, T.C., Hurlbert, R.J., Hadley, M.N., Aarabi, B., Dhall, S.S., Gelb, D.E., Rozzelle, C.J., Theodore, N., and Walters, B.C. (2013). The acute cardiopulmonary management of patients with cervical spinal cord injuries. Neurosurgery 72, 84–92.
6. Hawryluk, G. Whetstone, W., Saigal, R., Ferguson, A., Talbott, J., Bresnahan, J., Dhall, S., Pan, J., Beattie, M., Manley, G. (2015). Mean arterial blood pressure correlates with neurological recovery after human spinal cord injury: analysis of high frequency physiologic data. J. Neurotrauma 32, 1958–1967.
7. Macnab, A.J., Gagnon, R.E., Gagnon, F.A., LeBlanc, J.G. (2003). NIRS monitoring of brain and spinal cord—detection of adverse intraoperative events. Spectroscopy 17, 483–490.
8. Nielsen, H.B. (2014). Systematic review of near-infrared spectroscopy determined cerebral oxygenation during non-cardiac surgery. Front. Physiol. 5, 93.
9. Hamaoka, T.M., Niwayama, M., and Chance, B. (2011). The use of muscle near-infrared spectroscopy in sport, health and medical sciences: recent developments. Philos. Trans. A Math. Phys. Eng. Sci. 369, 4591–4604.
10. Delpy, D.T., Cope, M., van der Zee, P., Arridge, S., Wray, S., and Wyatt, J. (1988). Estimation of optical pathlength through tissue from direct time of flight measurements. Phys. Med. Biol. 33, 1433–1442.
11. Boushel, R., Langberg, H., Olesen, J., Nowak, M., Simonsen, L., Bülow, J., and Kjaer, M. (2000). Regional blood flow during exercise in humans measured by near-infrared spectroscopy and indocyanine green. J. Appl. Physiol. 89, 1868–1878.
12. Hagino, I., Anttila, V., Zurakowski, D., Duebener, L.F., Lidov, H.G., and Jonas, R.A. (2005). Tissue oxygenation index is a useful monitor of histologic and neurologic outcome after cardiopulmonary bypass in piglets. J. Thorac. Cardiovasc. Surg. 130, 384–392.
13. Matcher, S.J., Elwell, C.E., Cooper, C.E., Cope, M., and Delpy, D.T. (1995). Performance comparison of several published tissue near-infrared spectroscopy algorithms. Anal. Biochem. 227, 54–68.
14. Ferraris, A., Jacquet-Lagrèze, M., and Fellahi, J.L. (2018). Four-wavelength near-infrared peripheral oximetry in cardiac surgery patients: a comparison between EQUANOX and O3. Clin. Monit. Comput. 32, 253–259.
15. Wyser, D., Lambercy, O., Scholkmann, F., Wolf, M., and Gassert, R. (2017). Wearable and modular functional near-infrared spectroscopy instrument with multidistance measurements at four wavelengths. Neurophotonics 4, 041413.
16. Ferrari, M., Muthalib, M., and Quaresima, V. (2011). The use of near-infrared spectroscopy in understanding skeletal muscle physiology: recent developments. Philos. Trans. A. Math. Phys. Eng. Sci. 369, 4577–4590.
17. Macnab, A.J., and Shadgan, B. (2012). Biomedical applications of wireless continuous wave near infrared spectroscopy. Biomed. Spectrosc. Imaging 1, 205–222.
18. Lee, J.H., Streijger, F., Tigchelaar, S., Maloon, M., Liu, J., Tetzlaff, W., and Kwon, B.K. (2012). A contusive model of unilateral cervical spinal cord injury using the infinite horizon impactor. J. Vis. Exp. 24, 3313.
19. Strauch, J.T., Lauten, A., Zhang, N., Wahlers, T., and Griepp, R.B., (2007). Anatomy of spinal cord blood supply in the pig. Ann. Thorac. Surg. 83, 2130–2134.
20. Etz, C.D., Kari, F.A., Mueller, C.S., Silovitz, D., Brenner, R.M., Lin, H.M., and Griepp, R.B. (2011). The collateral network concept: a reassessment of the anatomy of spinal cord perfusion. J. Thorac. Cardiovasc. Surg. 141, 1020–1028.
21. Streijger, F., So, K., Manouchehri, N., Tigchelaar, S., Lee, J.H.T., Okon, E.B., Shortt, K., Kim, S.E., McInnes, K., Cripton, P., and Kwon, B.K. (2017). Changes in pressure, hemodynamics, and metabolism within the spinal cord during the first 7 days after injury using a porcine model. J. Neurotrauma 34, 3336–3350.
22. Schenkman, K.A. (2002). Visible and near infrared absorption spectra of human and animal haemoglobin. Crit. Care Med. 30, 267.
23. Tachtsidis. I., Tisdall, M.M., Leung, T.S., Pritchard, C., Cooper, C.E., Smith, M., and Elwell, C.E. (2009). Relationship between brain tissue haemodynamics, oxygenation and metabolism in the healthy human adult brain during hyperoxia and hypercapnea. Adv. Exp. Med. Biol. 645, 315–320.
24. Okon, E.B., Streijger, F., Lee, J.H.T., Anderson, L.M., Russell, A.K., and Kwon, B.K. (2013). Intraparenchymal microdialysis after acute spinal cord injury reveals differential metabolic responses to contusive versus compressive mechanisms of injury. J. Neurotrauma 30, 1564–1576.
25. Pollard, V., Prough, D.S., DeMelo, A.E., Deyo, D.J., Uchida, T., and Stoddart, H.F. (1996). Validation in volunteers of a near-infrared spectroscope for monitoring brain oxygenation in vivo. Anesth. Analg. 82, 269–277.
26. Ferrari, M., Binzoni, T., and Quaresima, V. (1997). Oxidative metabolism in muscle. Phil. Trans. R. Soc. Lond. B: Biol. Sci. 352, 677–683.

27. Shadgan, B., Guenette, J.A., Sheel, A.W., and Reid, W.D. (2011). Sternocleidomastoid muscle oxygenation and hemodynamic response to incremental inspiratory threshold loading measured by near infrared spectroscopy. Respir. Physiol. Neurobiol. 178, 202–209.
28. Kwon, B.K., Curt, A., Belanger, L.M., Bernardo, A., Chan, D., Markez, J.A., Gorelik, S., Slobogean, G.P., Umedaly, H., Giffin, M., Nikolakis, M.A., Street, J., Boyd, M.C., Paquette, S., Fisher, C.G., and Dvorak, M.F. (2009). Intrathecal pressure monitoring and cerebrospinal fluid drainage in acute spinal cord injury: a prospective randomized trial. J. Neurosurg. Spine 10, 181–193.
29. Pascual, J.L., Georgoff, P., Maloney-Wilensky, E., Sims, C., Sarani, B., Stiefel, M.F., LeRoux, P.D., and Schwab, C.W. (2011). Reduced brain tissue oxygen in traumatic brain injury: are most commonly used interventions successful? J. Trauma. 70, 535–546.
30. Stiefel, M.F., Spiotta, A., Gracias, V.H., Garuffe, A.M., Guillamondegui, O., Maloney-Wilensky, E., Bloom, S., Grady, M.S., and LeRoux, P.D. (2005). Reduced mortality rate in patients with severe traumatic brain injury treated with brain tissue oxygen monitoring. J. Neurosurg. 103, 805–811.

Address correspondence to:
Babak Shadgan, MD, MSc, PhD
International Collaboration on Repair Discoveries
Faculty of Medicine, Department of Orthopaedics
The University of British Columbia
5440 - ICORD, Blusson Spinal Cord Centre
818 West 10th Avenue
Vancouver, British Columbia V5Z 1M9
Canada

E-mail: shadgan@mail.ubc.ca